Continuous vortex pumping into a spinor condensate with magnetic fields

Z. F. Xu,[1] P. Zhang,[2,*] C. Raman,[2] and L. You[1,2]
[1]*Center for Advanced Study, Tsinghua University, Beijing 100084, People's Republic of China*
[2]*School of Physics, Georgia Institute of Technology, Atlanta, Georgia 30332, USA*
(Received 26 May 2008; published 9 October 2008)

We study the mechanisms and the limits of pumping vorticity into a spinor condensate through manipulations of magnetic (B) fields. We discover a fundamental connection between the geometrical properties of the magnetic fields and the quantized circulation of magnetically trapped atoms, a result that generalizes several recent experimental and theoretical studies. The optimal procedures are devised that are capable of continuously increasing or decreasing a condensate's vorticity by repeating certain two-step B-field manipulation protocols. We carry out detailed numerical simulations that support the claim that our protocols are highly efficient, stable, and robust against small imperfections of all types. Our protocols can be implemented experimentally within current technologies.

DOI: 10.1103/PhysRevA.78.043606 PACS number(s): 03.75.Lm, 03.75.Mn, 67.30.he, 73.43.−f

I. INTRODUCTION

A quantized vortex represents a hallmark of superfluidity [1]. The vorticity in a superfluid clearly reveals the topological nature associated with the phase of a condensate's wave function and has been studied extensively both theoretically and experimentally [1,2] since the first success of atomic Bose-Einstein condensation. In the strongly rotating limit when the number of vortices significantly exceeds the number of atoms, researchers have focused on the possibilities of observing interesting strongly correlated states [3–16].

Vortex states have been created experimentally relying on a variety of approaches: a spatially selective rotating Rabi coupling to an auxiliary internal state [17,18], stirring inside [19] or at the edge [20] of a condensate with a focused laser beam, rotating a deformed trap [21], or simply merging several condensate pieces [22] into a single trap. Other approaches include direct phase engineering through the imprinting of a nontrivial topological phase to the wave function of a condensate [23] using an azimuthal optical phase plate [24] or through manipulating external magnetic (B) fields [25–28]. Alternately, a condensate can gain angular momentum through its coupling to a Laguerre-Gaussian light beam [29–32] or other forms of gauge potentials [33].

The idea of phase imprinting from the nontrivial geometrical properties of external B fields is especially illuminating as it involves no forced rotation or essentially no spatial motion [25]. It has since been demonstrated in beautiful recent experiments [34–36]. The original protocol [25] involves an axially symmetric spinor condensate in the familiar B field of an Ioffe-Pritchard trap (IPT) [37] consisting of a two-dimensional (2D) quadrupole B field augmented by a bias B field along the symmetric z axis. Upon the flipping of the bias field, the adiabatically following weak field seeking state then develops a nonzero vorticity in its spatial wave function [25]. Our aim is to develop this protocol into a pump mechanism capable of continuously changing the vorticity of a condensate. The naive approach of repeated flips of the z-bias B field does not work because the second flip simply undoes the vorticity gained in the first flip, returning the condensate to the initial state.

Recently, Möttönen *et al.* [38] put forward an interesting idea that sought to break the time-reversal symmetry between the first and the second flips of the bias field. Their protocol starts with a 2D hexapole B field instead of a quadrupole field for the first flip. The hexapole field is then turned off and replaced by a quadrupole one for the second flip. It is known, as in the original bias flip protocol [25], that the first flip can generate a proportionally higher vorticity if the quadrupole is replaced by a higher-order 2D multipole such as a hexapole [39]. Repeating the two-step protocols with hexapole and quadrupole B fields in turn, Möttönen, *et al.* show that the vorticity increases by $4\hbar$ per atom in the hexapole step and decreases by $2\hbar$ per atom during the quadrupole step [38]. Thus each cycle composed of a bias flip with a hexapole field followed by a second bias flip with a quadrupole field increases the net vorticity by $4\hbar-2\hbar=2\hbar$. Higher vorticities are generated with repeated cycles.

A related earlier discussion [39] suggested an even simpler protocol of turning off the quadrupole field after the first flip, and then returning the axial bias field to its original direction. The return of the axial bias to the original direction is hoped to bring the system to the initial configuration except for the vorticity gained from the first flip. It was previously noted that by turning on the quadrupole field and repeating the above protocol, a continuous vortex pump is realized [39]. Unfortunately, no details were given on how the axial bias field is returned to the original direction [39]. Clearly it cannot be flipped back in the absence of the quadrupole field as the z-bias field remains aligned along the same axial direction. Simply letting it oscillate back with the axial B-field magnitude increasing from large negative to small negative, to zero, to small positive, and then finally to large positive values does not constitute a flip. Both the projections of mechanical angular momentum L_z and the spin $F_z(M_F)$ are independently conserved quantities during the above process.

*Present address: Tokyo Institute of Technology, Tokyo, Japan.

II. OUR CONTINUOUS VORTEX PUMP PROTOCOL

Our idea is physically intuitive and leads to a direct implementation for a continuous vortex pump with the introduction of an auxiliary transverse bias B field. As in a Stern-Gerlach experiment, the Zeeman population distribution inside an experimental apparatus can be measured along any quantization direction of a strong reference B field, provided the strong field is turned on adiabatically. When the transverse bias B field is pulsed on, it provides a reference direction for the axial bias field to flip back in the absence of the quadrupole field. We find it imperative to present this result because of the high interests stimulated by the recent work of Möttönen *et al.* [38]. Unlike Ref. [38], our proposal requires only one set of current coils capable of generating one type of multipole B field, be it a 2D quadrupole or a 2D hexapole. The time-reversal symmetry is broken in our protocol with the extra transverse bias B field, whose presence allows for the z-bias field to rotate instead of simply oscillating back.

As an illustration, we consider a spin-1 condensate in an IPT, whose B field is approximately $\vec{B}(x,y,z)=B'(x\hat{x}-y\hat{y})+B_z\hat{z}$ near the origin. Isoshima *et al.* [25] first discussed pumping vorticity into a condensate with external B fields. For a sufficiently large z-bias B field, a condensate of $F=1$ atoms adiabatically stays in the B-quantized $|M_F=-1,\vec{r}\rangle_B$ state. After an adiabatic flip of the bias field, a vortical phase structure or a vortex state is imprinted into the condensate [26–28,34–36]. The physics involved can be elucidated in terms of the symmetries and conservation laws of the model system [40] or from the gauge potential [41] due to the changing B field. More specifically, it is the conservation of D_z $(=L_z-F_z)$ that enables a straightforward understanding of the result of Isoshima *et al.* [25] in the axially symmetric IPT [42,43]. Each single flip of the bias field in the presence of a quadrupole field then imparts a $2F\hbar$ (for $F=1$ here) phase winding [25,34–36]. Repeated operations then constitute a continuous vortex pump [38]. As introduced above, our pump mechanism generalizes the original idea of Isoshima *et al.* [25]. Following the first flip, which imprints a $2\hbar$ vortex to the adiabatic state, we turn on a transverse bias field $B_x'\hat{x}$ and then continue with a second bias flip returning the system to the initial setup. A vortex pump then simply consists of repeated applications of the above manipulations to the three B fields: the 2D quadrupole, the axial bias, and the transverse bias fields.

The potential for high fidelity operation of our pump protocol is confirmed with numerical simulations for a spin-1 atomic condensate in external magnetic (B) fields. An additional optical trap $V_o=M\omega_\perp^2(x^2+y^2+\lambda^2z^2)/2$ provides a permanent confinement during the B-field manipulation. To avoid the energetic instability of the potential disintegration of a high vortex state into single vortices [50–52], we introduce an optical pinning plug $V_p(\rho,z,\phi)=U\exp(-\rho^2/2\rho_0^2)$ that expels atoms away from the low B-field region to assure adiabaticity. The force of gravity is assumed to be opposite to the axial z axis, which can be omitted in the approximate 2D treatment when the harmonic trap is taken to be pancake-shaped with $\lambda\gg1$. The z dependence is frozen in the ground state of the axial harmonic oscillator $\phi(z)$. Thus the vorticity is coded in the phase structures of the two-dimensional condensate wave function $\psi(\vec{\rho},t)$.

The condensate wave function thus becomes $\Psi(\vec{r},t)=\psi(\vec{\rho},t)\phi(z)$, where $\vec{\rho}=(x,y)$, $\phi(z)=(\lambda/\pi a_\perp^2)^{1/4}e^{-\lambda z^2/2a_\perp^2}$, and $a_\perp=\sqrt{\hbar/M\omega_\perp}$ is the length scale for the transverse harmonic trap. After integrating out the z coordinate, we obtain the effective 2D Gross-Pitaevskii equation

$$
\begin{aligned}
i\hbar\frac{\partial\psi_{\pm1}}{\partial t}&=[H_0+c_2^{(2D)}(n_{\pm1}+n_0-n_{\mp1})]\psi_{\pm1}+c_2^{(2D)}\psi_{\mp1}^*\psi_0^2\\
&\quad+H_{\pm10}^{ZM}\psi_0+H_{\pm1\mp1}^{ZM}\psi_{\mp1},\\
i\hbar\frac{\partial\psi_0}{\partial t}&=[H_0+c_2^{(2D)}(n_1+n_{-1})]\psi_0+2c_2^{(2D)}\psi_0^*\psi_1\psi_{-1}+H_{01}^{ZM}\psi_1\\
&\quad+H_{0-1}^{ZM}\psi_{-1},
\end{aligned}
\tag{1}
$$

where $H_0=-\frac{\hbar^2}{2M}\nabla_\perp^2+V_o^{2D}+V_p^{2D}+c_0^{2D}n$, $V_o^{2D}=\frac{1}{2}M\omega_\perp^2(x^2+y^2)$ and $V_p^{2D}=U\exp(-\rho^2/2\rho_0^2)$ are the 2D optical trap and optical plug, respectively. $n=\Sigma_i|\psi_i|^2$ is the 2D atom number density. The effective 2D spin-independent and spin-dependent interaction strengths are now characterized by $c_0^{(2D)}=2(2\pi\lambda)^{1/2}\hbar^2(a_0+2a_2)/3Ma_\perp$ and $c_2^{(2D)}=2(2\pi\lambda)^{1/2}\hbar^2(a_2-a_0)/3Ma_\perp$.

In the local B-quantized representation, the Zeeman energy is diagonal, given by the Breit-Rabi formula

$$
E_{M_F}=-\frac{\Delta E_0}{8}-M_Fg_I\mu_IB-\frac{\Delta E_0}{2}\sqrt{1+M_F\xi+\xi^2}. \tag{2}
$$

ΔE_0 is the hyperfine splitting. g_I is the Lande factor for the nuclear spin $\vec{I}$, μ_I is the nuclear magneton, and ξ is defined by $\xi=(g_I\mu_I+g_J\mu_B)B/\Delta E_0$. Here g_J is the Lande factor for the valence electron with total angular momentum $\vec{J}$, and μ_B is the Bohr magneton. Our Eq. (1) above requires Zeeman energy H^{ZM} of an atom in the laboratory based z-axis quantization representation that is nondiagonal and is given by $H^{ZM}=\mathcal{U}^\dagger E\mathcal{U}$ with $\mathcal{U}$ the unitary transformation connecting the z- and B-quantized representations. For the B field of an IPT, the transformation matrix becomes the product of two rotations in spin space, i.e., $\mathcal{U}=e^{iF_y\theta}e^{iF_z\phi}$, or in matrix form,

$$
\mathcal{U}=\begin{pmatrix}
\frac{1}{2}(1+\cos\theta)e^{i\phi} & \frac{1}{\sqrt{2}}\sin\theta & \frac{1}{2}(1-\cos\theta)e^{-i\phi}\\
-\frac{1}{\sqrt{2}}\sin\theta e^{i\phi} & \cos\theta & \frac{1}{\sqrt{2}}\sin\theta e^{-i\phi}\\
\frac{1}{2}(1-\cos\theta)e^{i\phi} & -\frac{1}{\sqrt{2}}\sin\theta & \frac{1}{2}(1+\cos\theta)e^{-i\phi}
\end{pmatrix}, \tag{3}
$$

with the rotation angles θ and ϕ introduced through the parametrization of the field $\vec{B}=B[\hat{z}\cos\theta+\sin\theta(\hat{x}\cos\phi+\hat{y}\sin\phi)]$. $H_{M_FM_F'}^{ZM}$ is one of the nine elements of H^{ZM} with spinor components ordered as $M_F=1,0,-1$.

Our numerical simulations assume a condensate of $N=10^5$, ^{87}Rb atoms in the $F=1$ state and trapped as described above with $\lambda=100$. We take $\omega_\perp=2\pi\times30$ Hz, $U/\hbar=2$

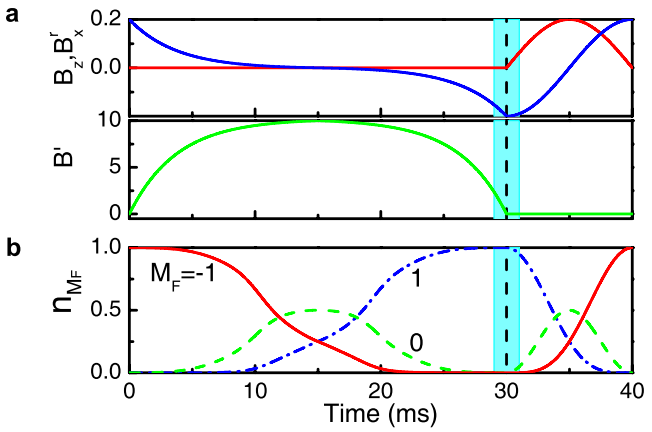

FIG. 1. (Color online). (a) The time dependence of the B fields. In the first 30 ms, B_z decreases to the opposite of the initial value. The gradient increases from 0 to the maximum in 15 ms, then decreases to zero. Next, the B field is rotated back, while a uniform transverse bias in the x-axis direction is pulsed on for the latter 10 ms, keeping the $B_z^2+(B_x^r)^2$ a constant. (b) The time-dependent fractional population $n_{M_F}=N_{M_F}/N$ in the Zeeman state.

$\times 10^5$ Hz, and $\rho_0=5$ μm. The B field takes a form $\vec{B}=B'(x\hat{x}-y\hat{y})+B_z\hat{z}+B_x^r\hat{x}$ with a typical temporal evolution within one period as illustrated in Fig. 1. During the first 15 ms, we decrease B_z and increase B' according to the following easily programmed time dependence:

$$B_z(t)=B_z(0)(e^{-8t/T_1+2}-e^{-2})/(e^2-e^{-2}), \tag{4}$$

$$B'(t)=B'(T_1/2)(e^2-e^{-8t/T_1+2})/(e^2-e^{-2}), \tag{5}$$

with $T_1=30$ ms. In the subsequent 15 ms, B_z is decreased continuously as is the gradient B'. Both time dependences are relatively smooth and of an exponential type similar to the first 15 ms. The time dependence of the z-bias flip and the transverse x-bias pulse on are described by

$$B_z(t)=B_z(0)\cos\{\pi[1-(t-T_1)/T_2]\}, \tag{6}$$

$$B_x^r(t)=B_z(0)\sin\{\pi[1-(t-T_1)/T_2]\}, \tag{7}$$

with $T_2=10$ ms. Due to the adiabatic nature of our proposed protocol, the quality of the final result or the fidelity of the intended vortex state do not sensitively depend on the details of the time dependence of the B fields, provided they are reasonably smooth functions of time. In the shadow window of Fig. 1, nothing really happens to the condensate spinor component population distribution as long as the B fields change smoothly. Because B_z is much larger than the field due to the gradient B' within this window, the angle between the net B field and the z axis remains small even for a discontinuous change of the bias field or the quadruple gradient, causing the atomic spin state to change smoothly. Depending on the net radial trap strength from the combined trap and the optical plug, the azimuthal vortical phase distribution changes with the radius due to nonadiabatic effects with respect to the radial motional state.

In all of our simulations, the initial state is obtained from the imaginary time propagation of the coupled Gross-Pitaevskii equations with an initial Gaussian wave function in the $M_F=-1$ state setting $c_2=0$ and with no B field as discussed in the supplementary material. The vortex pump protocol is then simulated in real time. For the case of a 2D quadrupole, the first flip of the bias B_z from 0.2 to -0.2 G is carried out in the first 30 ms, along with the increasing of the B-field gradient B' to the maximum value of 10 G/cm and followed with a gradual switch off. In the following 10 ms, the bias field is rotated back around the y axis in the x-z plane, aided by the transverse bias field along the x axis. Similar steps are involved when the 2D quadrupole is replaced by a 2D hexapole. In Fig. 2, we show the temporal development of the phase structures for the $M_F=1$ component after the first B_z flip and the $M_F=-1$ component after the next flip back to the original direction for the first five repetitions. The total vorticity changes are impressive and confirm conclusively our suggested protocol for a continuous vortex pump applied with a hexapole. For a quadrupole field, we find essentially the same quality operation, except that each repetition adds $2\hbar$ units of vorticity as compared to $4\hbar$ units for a hexapole (Fig. 2). More generally with a z-bias field along the symmetry axis of a $2l$th multipole 2D B field $\vec{B}\propto\rho^{l-1}[\cos(l\phi)\hat{\rho}-\sin(l\phi)\hat{\phi}]$, $D_z=L_z-(l-1)\times F_z$ is conserved for the symmetric ground condensate state [40]. A corresponding adiabatic flip of the bias field is thus capable of generating a $2(l-1)F\hbar$ vortex.

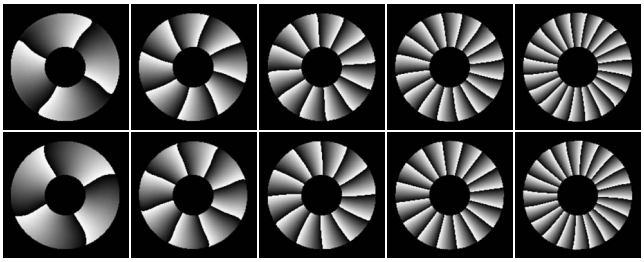

FIG. 2. The temporal development of the condensate phase structures in a hexapole field $\vec{B}_h=B_h'[(x^2-y^2)\hat{x}-2xy\hat{y}]$ plus a transverse bias field $B_x^r\hat{x}$. The upper row shows the $M_F=1$ component at the end of the first flips, or in the middle of each cycle at 30, 70, 110, 150, and 190 ms, respectively; the lower row is for the $M_F=-1$ state at 10 ms later with respect to the first row or at the end of each cycle at 40, 80, 120, 160, and 200 ms. The temporal dependence of the B fields and other parameters are as in Fig. 1 of the supplementary material. The maxima for B_h', B_z, and B_x^r are 1250 G/cm^2, 0.1, and 0.1 G, respectively. White (black) color denotes phase $-\pi$ (π).

Before providing the general considerations that will lead to our discovery of the optimal vortex pump protocols based on manipulating external B fields, we provide further numerical studies that demonstrate the efficiency, stability, and robustness of our vortex pump protocol.

First, we discuss the relatively relaxed conditions on adiabaticity for the manipulation of the external B field. Typically, the z-bias field is flipped over during a time of 30 ms in our numerical simulations, although we find integer numbers of vorticity are still created provided the flipping time is adjusted considerably (shorter or longer). Due to the symmetries and the corresponding conservation laws on the dynam-

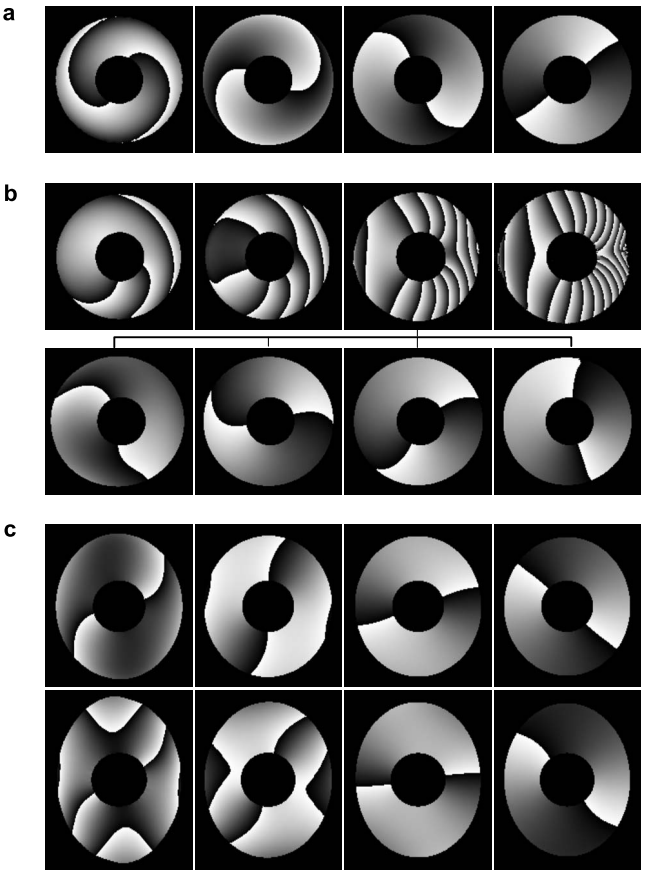

FIG. 3. The condensate phase distribution for the $M_F=1$ state after flipping the z bias in an IPT. (a) The ideal case of an IPT with perfect alignment with the optical trap and the plug. The flip times are 30, 60, 90, and 120 ms from the left to the right, accompanied by an increasing level of adiabaticity. (b) The same as in (a) except for a misaligned optical plug $V_p^{2D}=U\exp\{-[(x-x_0)^2+y^2]/2\rho_0^2\}$, $U/\hbar=2\times10^5$ Hz, and $\rho_0=5$ μm. From the left to the right in the upper row, the results are compared for $x_0/\rho_0=0.05$, 0.1, 0.2, and 0.3, respectively, at a bias flip time of 30 ms. In the lower row $x_0=0.2\rho$, where results from different flip times of 60, 90, 120, and 150 ms are compared from the left to the right. (c) The same as in (a) except for a non-axial-symmetric optical trap $V_o^{2D}=M\omega_\perp^2[(1+\varepsilon)^2x^2+(1-\varepsilon)^2y^2]/2$ parametrized by ε. The upper row is for $\varepsilon=0.05$, and $\varepsilon=0.1$ in the lower row. The z-bias flipping times used are 60, 90, 120, and 210 ms from left to right, respectively.

ics of our model system—the conservations of $D_z=L_z-F_z$ in an IPT, L_z+F_z in a 3D quadrupole trap (QT), and $L_z-(l-1)F_z$ in a $2l$th multipole 2D B field high-fidelity operations are assured even with marginal conditions for adiabaticity. On careful examination, we find that the aximuthal distributions of the phases are complicated, not the simple linear dependence one might have imagined. Instead, the dependence on the azimuthal angle is different at a different radial coordinate, indicating a violation of the adiabatic condition with respect to the radial motional state. However, as long as the internal state can follow adiabatically the flipping z-bias B field, our intuitive vortex pump protocol remains effective. As we demonstrate in Fig. 3(a), for successive flipping times of 30 ms to 60, 90, and 120 ms, the phase distribution approaches the same form with the increasing level of adiabaticity.

Next, we study the effect of misalignment of the axial symmetric optical trap with respect to the geometric center of the external B field. Any misalignment will reduce the axial symmetry, and thus break the angular momentum conservation law [40] and adversely impact the quality of our vortex pump protocol. Without loss of generality, we assume the optical plug's center is $(x_0,0,0)$ while other symmetries are assumed to remain. After extensive numerical simulations as before, we find that a misalignment of the percent level of the transverse size for the condensate is already detrimental to the pump protocol as shown in the upper row of Fig. 3(b) when the bias flip time is 30 ms. More generally, we find that the larger x_0 is, the stronger is the deviation from the intended vortical phase distribution pattern. Somewhat surprisingly, however, we find a simple solution to this ailment. By increasing the z-bias flip time, the complicated phase structures disappear gradually as shown in the lower row of Fig. 3(b), where the flip time is taken to be 60, 90, 120, and 150 ms from left to right. These results show that unless there is a total failure in aligning the optical trap with respect to the B-field trap, the nominally small misalignment can be compensated for by the proposed vortex pump protocol with a correspondingly slower flipping time.

Finally, we study the potential degradation due to an asymmetric optical trap. As with the misalignment considered above, an asymmetric optical trap will void the conservation of D_z. Although the intended adiabatic manipulation of the B field can still transform all atoms from the $M_F=-1$ to 1 spin state and cause the F_z to change from $-\hbar$ to $\hbar$ for a spin-1 condensate, the axial motional angular momentum per atom gained will not be equal to $2\hbar$, except when the asymmetry is small. Instead, L_z is generally found to oscillate near the end of the B field flipping, as we show in Fig. 4. For relatively small trap anisotropy, for instance at $\varepsilon=0.05$, the vortex generated is not far away from the ideal case of perfect symmetry. This can be readily derived from the axial angular momentum shown in Fig. 4(a) or by comparing the condensate's phase structure in Fig. 3(c) with Fig. 3(a). With larger optical trap asymmetries, for example at the threshold of $\varepsilon=0.1$ for the system and parameters that we consider, the average angular momentum per particle (L_z) gained by the condensate is no longer an integer multiple of $\hbar$. The condensate phase structure becomes more complicated at short flip times, and if the optical trap asymmetry is distorted further, a dynamical instability begins to set in within the same evolution time. Based on our numerical simulations, when $\varepsilon=0.125$ and the flipping time is set to 30 ms, a dynamical instability occurs. In addition, we find significant blurring in the condensate density distribution after flipping the B field. The phase difference between nearby spatial positions is totally smeared out. As the flipping time is increased further, dynamical instability or the blurring disappears while a high-quality winding pattern reemerges. Our simulations also show that the dynamical instability survives at larger rotations for smaller trap asymmetries.

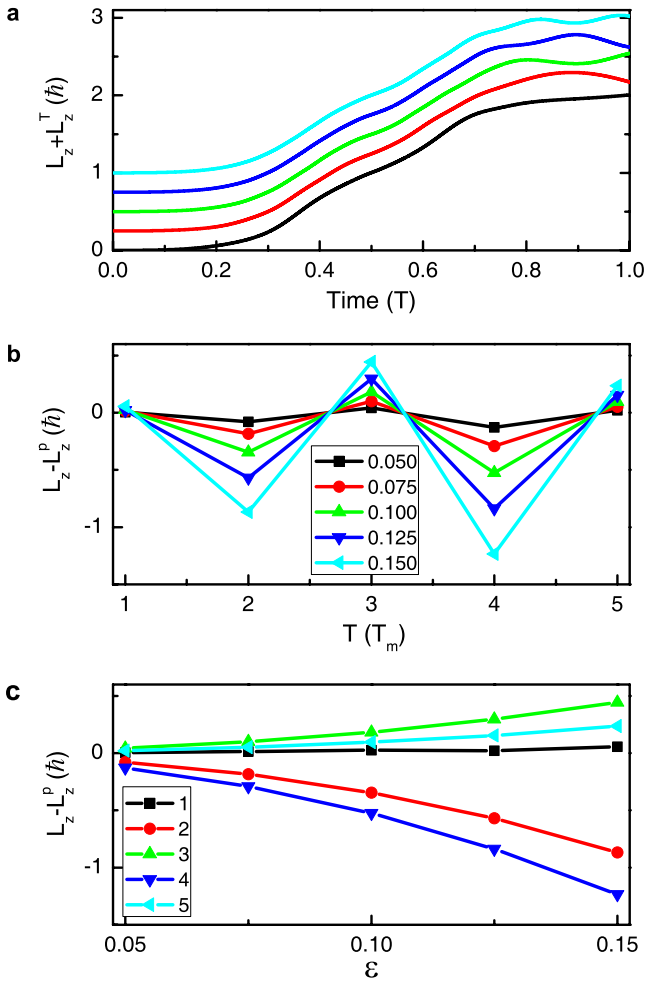

FIG. 4. (Color online). The motional angular momentum gained with our protocol in an asymmetric optical trap and an IPT. (a) The temporal development of L_z during the flip of the z-bias field at an asymmetry parameter $\varepsilon=0.05$. The flip time T is 30, 60, 90, 120, and 150 ms, respectively, and is shown by offset lines from the lower to the higher. The offset shift for each curve is given by $L_z^T=0.25\hbar\times[(T/T_m)-1]$, and $T_m=30$ ms. (b) The difference between angular momentum gained from our protocol in an asymmetric optical trap with $L_z^p=2\hbar$ predicted for the ideal case. The curves denote different asymmetry parameter ε from 0.05 to 0.15 as shown by the inset labels. (c) The same as in (b), but now for the ε dependence at the same flip time T. The five curves are labeled by their respective T/T_m values from 1 to 5.

III. GEOMETRICAL PROPERTIES OF STATIC MAGNETIC FIELDS

According to Maxwell's equation, the spatial distribution of a static B field can be expressed as the gradient of a scalar potential $\Phi(\vec{r})$, i.e.,

$$\vec{B}(\vec{r})=[B_x(\vec{r}),B_y(\vec{r}),B_z(\vec{r})]=\nabla\Phi(\vec{r}). \tag{8}$$

Since the divergence of a static B field is always zero, or $\nabla\cdot\vec{B}=\mathbf{0}$, the scalar potential satisfies the Laplace equation $\nabla^2\Phi(\vec{r})=\mathbf{0}$. Thus $\Phi(\vec{r})$ can be expanded in terms of the spherical harmonic functions, to

$$\Phi(\vec{r})=\sum_{lm} c_{lm}r^l P_l^m(\cos\theta)e^{im\phi}, \tag{9}$$

in the spherical coordinate (r,θ,ϕ).

The vortex pump protocol we proposed relies on the repeated flips of the z-bias field B_z adiabatically from the $+z$ to the $-z$ direction and vice versa. The vorticity gained by a condensate can be understood in terms of the conservations of D_z or L_z+F_z, which are ultimately determined by the angle ϑ between $\vec{B}(\vec{r})$ and the x axis (or the y axis). A vortex state has a two-dimensional phase structure. For a stable vortex state with its angular momentum pointed along the z axis, the velocity $\vec{v}=\frac{\hbar}{M}\nabla\phi_p$ must flow along the same azimuthal direction, and the phase ϕ_p in any plane with $z=z_0$ must be similar to that in the $z=0$ plane, i.e., $\phi_p(\rho,z,\phi)=\phi_p(\rho,0,\phi)+f(z)$. To effectively obtain a stable vortex state, the angle ϑ should (i) depend only on ϕ but remain independent of z, i.e., $\vartheta(\rho,z,\phi)=\vartheta(\rho,0,\phi)$; or (ii) depend on both ϕ and z but take the form $\vartheta(\rho,z,\phi)=\vartheta(\rho,0,\phi)+g(z)$. These constrains then lead to the condition

$$c_{lm}=0, \tag{10}$$

where $m\neq\pm l$ or $m\neq 0$ on the expansion coefficients. To obtain a vortex state with a definite winding number, the scalar potential thus has to take one of the following two possible forms:

$$\Phi_l^{(\mathrm{I})}(\vec{r})\propto\rho^l\cos(l\phi+\eta) \tag{11}$$

or

$$\Phi^{(\mathrm{II})}(\vec{r})=\sum_l c_l r^l P_l^0(\cos\theta), \tag{12}$$

where (ρ,z,ϕ) are the cylindrical coordinates and η is a constant angle. In the derivation of the second form, we have used the fact that $\Phi(\vec{r})$ is real.

In the first case above and as was discussed in the thesis work of Leanhardt [39], the B field takes the form

$$\vec{B}_l^{(\mathrm{I})}(\vec{r})\propto\rho^{l-1}[\cos(l-1)\phi\hat{e}_x-\sin(l-1)\phi\hat{e}_y], \tag{13}$$

with $l\geqslant 2$. The corresponding conserved quantity becomes $D_z=L_z-(l-1)\times F_z$. When $l=2$, this is the field of an IPT. In the work of Möttönen [38], both fields $\vec{B}_3^{(\mathrm{I})}(\vec{r})$ of a hexapole and $\vec{B}_2^{(\mathrm{I})}(\vec{r})$ of a quadrupole are used. For a spin-1 condensate, the vorticity gained is $L_z=2(l-1)\hbar$ after adiabatically flipping the $B_z(\vec{r})$.

In the second case, the simplest B field is

$$\vec{B}^{(\mathrm{II})}(\vec{r})=B_\rho(\vec{r})\hat{e}_\rho+B_z(\vec{r})\hat{e}_z, \tag{14}$$

as in a 3D QT. In the x-y plane, $\vec{B}^{(\mathrm{II})}$ points along the direction of $\hat{e}_\rho$. For a spin-1 condensate, the vorticity gained is $L_z=-2\hbar$ per atom after the flipping of $B_z(\vec{r})$. For completeness, we have confirmed this numerically for a 3D quadrupole trap. A slight complication arises in this case, as the B field depends on the z coordinate, and its zero-value point moves from $-\infty$ to $+\infty$ during the flipping of the z bias from -0.1 to 0.1 G. To demonstrate the numerics, we used the coupled 3D Gross-Pitaevskii equations. The gain of an

$L_z=-2\hbar$ vortex also can be understood in this case as being due to the conservation of F_z+L_z [40].

IV. THE OPTIMAL VORTEX PUMP PROTOCOL

As discussed above in some detail, starting in the initial spin state $|(-1)\rangle_z$, vorticity can be pumped into the motional state of a condensate if the z-bias field B_z is flipped from the positive to the negative z axis. When the static field is of the form $\vec{B}_l^{(\mathrm{I})}(\vec{r})$, the vortex state has $L_z=2(l-1)\hbar$; if the form is changed to $\vec{B}^{(\mathrm{II})}(\vec{r})$, a vortex state of $L_z=-2\hbar$ is obtained. The geometrical constraint on a static B field together with its coupling to the atomic hyperfine spin stops the change of the atom's internal state through the flipping of the z-bias B field. In fact, the opposite vortex state of $-2(l-1)\hbar$ with $l\geqslant 3$ can never be created through the flipping of B_z associated with any B field. Clearly, our studies provide an optimal vorticity pumping protocol based on a cyclic flipping of the bias B_z field as devised below.

If we have access only to the field $\vec{B}_l^{(\mathrm{I})}(\vec{r})$, we can turn it on and generate a vortex with $L_z=2(l-1)\hbar$ through the flipping of the bias in the first step. Then, this is followed by a second step where the field $\vec{B}_l^{(\mathrm{I})}(\vec{r})$ is turned off, and the bias field B_z is flipped back with the help of a constant transverse bias $B_x^r\hat{x}$, as we have suggested. The second step does not create any vorticity but returns the internal state to what it was initially. Repeating the two-step protocols, we pump $L_z=2(l-1)\hbar$ units of vorticity into the condensate for each cycle. The motional angular momentum gained from this protocol for the first five repetitions is shown in Fig. 6(a).

If we have access to both fields $\vec{B}_l^{(\mathrm{I})}(\vec{r})$ and $\vec{B}^{(\mathrm{II})}(\vec{r})$, the second step of each cycle is modified by tuning on the field $\vec{B}^{(\mathrm{II})}(\vec{r})$, which gains an additional $2\hbar$ units of vorticity in each cycle, for a total of $2l\hbar$ angular momentum gained per cycle. Figure 6(b) shows the continuously increasing vorticity for this more general case of the two type 2D multipole fields with $l=3$ and 2.

Finally, in light of our analysis above, the protocol devised in Ref. [38], which uses only the field of $\vec{B}_l^{(\mathrm{I})}(\vec{r})$ with $l=3$ and 2, respectively, in the first and the second steps of each cycle, is clearly not optimal. In the first step, the condensate gains a vorticity of $4\hbar$, while in the second step, it gains a vorticity of $-2\hbar$, or loses $2\hbar$. In the end, the net gain is only a $2\hbar$ per cycle. We summarize the various vortex pump protocols based on the manipulations with external B fields in Fig. 5.

In actual experiments, many complications could arise that make the selection of the optimal vortex pump protocol an entirely system-dependent matter. For instance, the loss of atoms and quantum coherence due to dissipation or decoherence strongly limit the lifetimes of all currently available atomic superfluids. If the criterion for the optimal protocol is defined as the maximal amount of vorticity gained during a fixed time, our analysis above then points to a clear winner: the repeated applications with only the hexapole field $\vec{B}_3^{(\mathrm{I})}(\vec{r})$ as evidenced by the results in the illustrated figures above.

Before concluding, we want to point out that D_z remains conserved within our formulation using the exact eigenenergies for the three Zeeman states, which is indeed confirmed in numerical simulations. This is easily understood because the effective Zeeman interaction $H^{\mathrm{ZM}}=E_0-\eta_0\vec{F}\cdot\vec{B}/B+\delta(\vec{F}\cdot\vec{B})^2/B^2$ with $\eta_0=(E_{-1}-E_1)/2$ and $\delta=(E_1+E_{-1}-2E_0)/2$ commutes with D_z. In addition, L_z is also conserved during the 10 ms intervals when only a uniform B field is present.

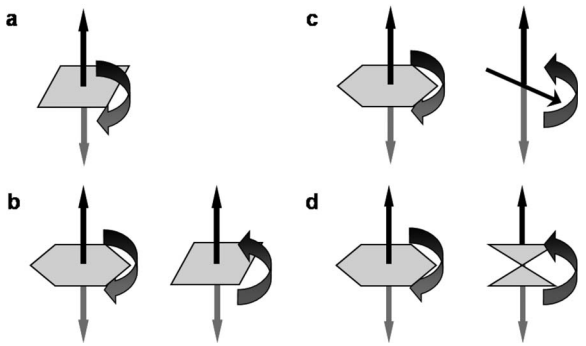

FIG. 5. Different vortex pump protocols compared, from the top to the bottom. The parallelogram and hexagon denote, respectively, 2D quadrupole and hexapole B fields, and the stacked pyramids denote a 3D quadrupole B field. The initial z bias is denoted by the solid black line arrow that is flipped to the opposite direction denoted by gray line arrow in the first step; the slanted solid black line arrow in the right figure of (c) refers to the transverse bias. (a) The original theoretical protocol of Ref. [25], which has been experimentally demonstrated [34–36], can pump only once. (b) The continuous pump protocol of Ref. [38]. It works, but the condensate vorticity does not change monotonically; (c) and (d) are the optimal protocols we discuss. They are capable of continuous and monotonic changes to the vorticity of a condensate. They are the optimal protocols based on the manipulation of B fields.

V. CONCLUSION

In conclusion, we have proposed and demonstrated numerically a simple yet efficient vortex pump protocol capable of continuously increasing or decreasing the vorticity of a condensate through repeated manipulations of external B fields: a bias along the axial direction, a 2D quadrupole field or hexapole field, and a 3D quadrupole field or a transverse bias field. Based on a general consideration of the geometrical properties of static B fields, we have shown that the above choices of B fields are the only possibilities capable of continuously controlling angular momentum vorticity in a spinor condensate through the manipulation of B fields. In Fig. 6, we compare the two optimal protocols for continuously increasing vorticity for the first five repetitions. The vorticity is seen increasing to $20\hbar$ and $10\hbar$ by using only $\vec{B}_l^{(\mathrm{I})}(\vec{r})$ for a hexapole ($l=3$) and a quadrupole ($l=2$), respectively, in (a), and to $30\hbar$ and $20\hbar$ by combining both $\vec{B}_l^{(\mathrm{I})}(\vec{r})$ and $\vec{B}^{(\mathrm{II})}(\vec{r})$ for $l=3$ and 2, respectively, in (b). To assure adiabaticity throughout the B-field manipulations, each cycle has to be engineered differently in the two protocols. For the first protocol as shown in (a), the duration for each cycle or its period is $T_1=40$ ms. During the first 30 ms, we use $\vec{B}_l^{(\mathrm{I})}(\vec{r})$

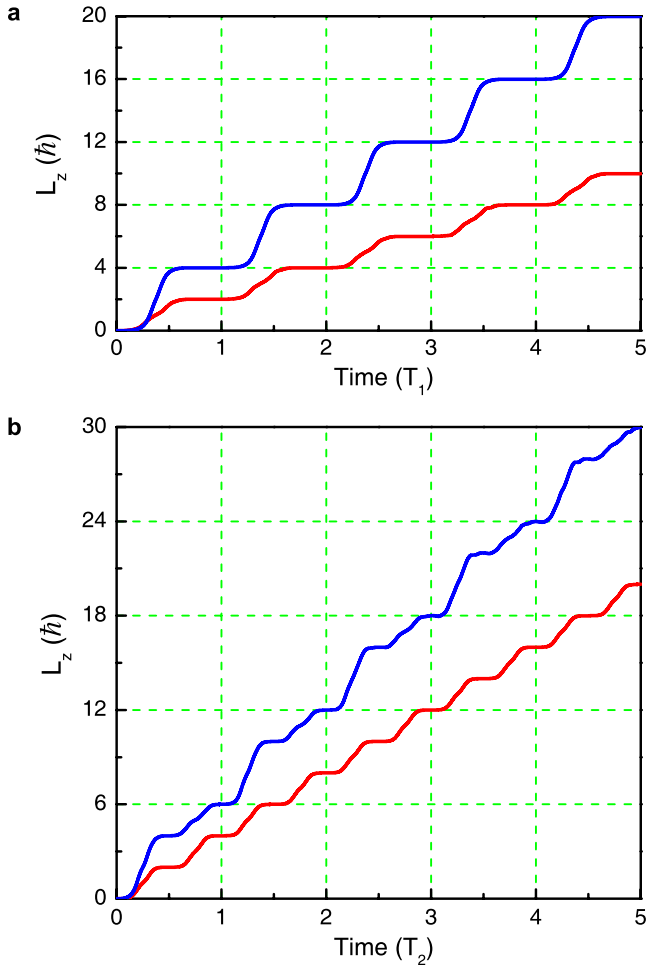

FIG. 6. (Color online). The continuously increasing vorticity of a condensate for the optimal protocols. (a) With only $\vec{B}_l^{(\mathrm{I})}(\vec{r})$ for a hexapole ($l=3$ the upper blue curve) and a quadrupole ($l=2$ the lower red curve). $T_1=40$ ms is the time of flipping. In the first 30 ms, $\vec{B}_l^{(\mathrm{I})}(\vec{r})$ is turned on to gain vorticity, while no vorticity is gained in the following 10 ms when a transverse bias along the x axis is turned on to reset the internal states to be as they were initially. (b) With both B fields $\vec{B}_l^{(\mathrm{I})}(\vec{r})$ ($l=3$ for the upper blue curve and $l=2$ for the lower red curve) and $\vec{B}^{(\mathrm{II})}(\vec{r})$ available and used for the first and second steps, respectively, of each cycle. $T_2=60$ ms is the total time for each cycle. In the first 30 ms $\vec{B}_l^{(\mathrm{I})}(\vec{r})$ is present, and in the next 30 ms $\vec{B}^{(\mathrm{II})}(\vec{r})$ is turned on while $\vec{B}_l^{(\mathrm{I})}(\vec{r})$ is turned off. The vorticity increases at all times in this case. The dashed lines in the two figures are guides for the eye.

to increase vorticity, and in the following 10 ms the transverse bias along the x axis is turned on to reset to the initial internal state through a second z-bias flip. For the second protocol of (b), the period required becomes $T_2=60$ ms. During the first 30 ms $\vec{B}_l^{(\mathrm{I})}(\vec{r})$ is present and in the following 30 ms $\vec{B}^{(\mathrm{II})}(\vec{r})$ is turned on while $\vec{B}_l^{(\mathrm{I})}(\vec{r})$ is turned off.

Our discussions indicate that for $l=2$, the second protocol is more efficient if a maximal amount of vorticity is sought, while for $l=3$, our results show that the efficiencies for the two protocols are about the same due to the different time requirements for adiabaticity. Based on the experience from the numerical simulations and from experimental works, it seems more practical to use the first protocol. The reason is rather simple, it is always more difficult to have two types of magnetic traps (from two sets of current-carrying coils) working together. The first protocol requires only one type of multipole 2D B field $\vec{B}_l^{(\mathrm{II})}(\vec{r})$, that can be realized on an atom chip [44], using a three-or four-wire structure for a 2D QT [45], or a five-wire structure for a 2D hexapole trap [46].

We demonstrate above the practical limit of reaching $30\hbar$ per atom using our protocol, which is already much larger than anything reported experimentally through the stirring of a condensate. We do not know what the maximum limit is. In fact, the exact value of this maximum is perhaps not so important either for two reasons: (i) our theory is mean field and may well break down at such larger angular momentum per atom because quantum correlations become essential; (ii) we are also limited by the computational resources available for such large-scale simulations.

The prospect for realizing the proposed vortex pump mechanism provides new impetus to active pursuits of quantum simulations of strongly interacting many-body electronic systems in terms of cold atoms [3–16]. It opens new avenues of theoretical and experimental research into the coupling between the internal and motional degrees of freedom and shines new light on relevant topics in spintronics studies [47].

Finally, we note that in all our protocols discussed above, there always exist a conserved quantity D_z for the ideal case of the model system. To create a vortex, one simply needs to adiabatically flip the B field to transfer all atoms from the weak field seeking Zeeman state $|-1\rangle_z$ to $|+1\rangle_z$, or the reverse. An obvious connection can be made with the famous Einstein–de Haas effect to deepen the understanding of our protocol and to possibly extend to the systems of dipolar quantum gases [48,49]. During our extensive numerical simulations, we find that a small B-field gradient B' or B_h', combined with a stronger optical plug, enforces the stability of the high vorticity states as generated. As is well known, high-order multipole B-field traps are usually not ideal candidates for magnetic traps because they are too weak to trap atoms. As far as vortex pump is concerned, however, a hexapole trap is preferred over a quadrupole trap because we are making use the topological structure of the B field, rather than its spatial dependence when trapping is considered.

To help with further experimental effort, we suggest a feasible implementation scheme on an atom chip. As is well known, an IPT can be realized by combing a chip based Z-type trap with a constant B field [44]. This type of IPT is not an ideal setup for implementing our protocols because the locations of trap zeros at the vanishing B field change following increasing or decreasing currents in the on-chip wires. The IPTs from the more stable three-or four-wire structures, on the other hand, are more promising candidates as evidenced by their demonstrated successes and stabilities in our chip matter wave manipulations [45]. For the three-wire structure, three equally spaced parallel wires lay on the surface of an atom chip, with the current in the middle wire opposite to the other two side wires. The four-wire structures

are analogously configured. Following similar ideas, a two-dimensional hexapole trap can be constructed by five wires [46]. Additionally these chip-based traps can be combined with optical traps, such as an optical plug, to realize a rich variety of confinement geometries. The force of gravity can be made to align along any of the symmetry axes of the two-dimensional multipole trap or compensated with an additional optical confinement.

ACKNOWLEDGMENTS

This work was supported by the U.S. NSF, and NSFC and MOST of China. C.R. acknowledges support from ARO.

[1] A. J. Leggett, Rev. Mod. Phys. **73**, 307 (2001).
[2] A. Fetter and A. Svidzinsky, J. Phys.: Condens. Matter **13**, R135 (2001).
[3] G. F. Bertsch and T. Papenbrock, Phys. Rev. Lett. **83**, 5412 (1999).
[4] A. D. Jackson and G. M. Kavoulakis, Phys. Rev. Lett. **85**, 2854 (2000).
[5] A. D. Jackson, G. M. Kavoulakis, B. Mottelson, and S. M. Reimann, Phys. Rev. Lett. **86**, 945 (2001).
[6] B. Paredes, P. Fedichev, J. I. Cirac, and P. Zoller, Phys. Rev. Lett. **87**, 010402 (2001).
[7] T. L. Ho, Phys. Rev. Lett. **87**, 060403 (2001).
[8] N. R. Cooper, N. K. Wilkin, and J. M. F. Gunn, Phys. Rev. Lett. **87**, 120405 (2001).
[9] J. Sinova, C. B. Hanna, and A. H. MacDonald, Phys. Rev. Lett. **89**, 030403 (2002).
[10] G. Watanabe, G. Baym, and C. J. Pethick, Phys. Rev. Lett. **93**, 190401 (2004).
[11] M. A. Baranov, K. Osterloh, and M. Lewenstein, Phys. Rev. Lett. **94**, 070404 (2005).
[12] V. Schweikhard, I. Coddington, P. Engels, V. P. Mogendorff, and E. A. Cornell, Phys. Rev. Lett. **92**, 040404 (2004).
[13] V. Bretin, S. Stock, Y. Seurin, and J. Dalibard, Phys. Rev. Lett. **92**, 050403 (2004).
[14] M. W. Zwierlein, J. R. Abo-Shaeer, A. Schirotzek, C. H. Schunck, and W. Ketterle, Nature (London) **435**, 1047 (2005).
[15] C. Ryu, M. F. Andersen, P. Clade, V. Natarajan, K. Helmerson, and W. D. Phillips, Phys. Rev. Lett. **99**, 260401 (2007).
[16] A. G. Morris and D. L. Feder, Phys. Rev. Lett. **99**, 240401 (2007).
[17] M. R. Matthews, B. P. Anderson, P. C. Haljan, D. S. Hall, C. E. Wieman, and E. A. Cornell, Phys. Rev. Lett. **83**, 2498 (1999).
[18] J. E. Williams and M. J. Holland, Nature **401**, 568 (1999).
[19] S. Inouye, S. Gupta, T. Rosenband, A. P. Chikkatur, A. Gorlitz, T. L. Gustavson, A. E. Leanhardt, D. E. Pritchard, and W. Ketterle, Phys. Rev. Lett. **87**, 080402 (2001).
[20] K. W. Madison, F. Chevy, W. Wohlleben, and J. Dalibard, Phys. Rev. Lett. **84**, 806 (2000).
[21] E. Hodby, G. Hechenblaikner, S. A. Hopkins, O. M. Maragò, and C. J. Foot, Phys. Rev. Lett. **88**, 010405 (2001).
[22] D. R. Scherer, C. N. Weiler, T. W. Neely, and B. P. Anderson, Phys. Rev. Lett. **98**, 110402 (2007).
[23] Ł. Dobrek, M. Gajda, M. Lewenstein, K. Sengstock, G. Birkl, and W. Ertmer, Phys. Rev. A **60**, R3381 (1999).
[24] J. Denschlag *et al.*, Science **287**, 97 (2000).
[25] T. Isoshima, M. Nakahara, T. Ohmi, and K. Machida, Phys. Rev. A **61**, 063610 (2000).
[26] M. Nakahara, T. Isoshima, K. Machida, S.-I. Ogawa, and T. Ohmi, Physica B **284-288**, 17 (2000).
[27] S.-I. Ogawa, M. Möttönen, M. Nakahara, T. Ohmi, and H. Shimada, Phys. Rev. A **66**, 013617 (2002).
[28] M. Möttönen, N. Matsumoto, M. Nakahara, and T. Ohmi, J. Phys.: Condens. Matter **14**, 13481 (2002).
[29] K.-P. Marzlin, W. Zhang, and E. M. Wright, Phys. Rev. Lett. **79**, 4728 (1997).
[30] E. Bolda and D. Walls, Phys. Lett. A **246**, 32 (1998).
[31] R. Dum, J. I. Cirac, M. Lewenstein, and P. Zoller, Phys. Rev. Lett. **80**, 2972 (1998).
[32] G. Nandi, R. Walser, and W. P. Schleich, Phys. Rev. A **69**, 063606 (2004).
[33] D. R. Murray, S. M. Barnett, P. Öhberg, and D. Gomila, arXiv:0709.0895.
[34] A. E. Leanhardt, A. Gorlitz, A. P. Chikkatur, D. Kielpinski, Y. Shin, D. E. Pritchard, and W. Ketterle, Phys. Rev. Lett. **89**, 190403 (2002).
[35] A. E. Leanhardt, Y. Shin, D. Kielpinski, D. E. Pritchard, and W. Ketterle, Phys. Rev. Lett. **90**, 140403 (2003).
[36] M. Kumakura, T. Hirotani, M. Okano, Y. Takahashi, and T. Yabuzaki, Phys. Rev. A **73**, 063605 (2006).
[37] D. E. Pritchard, Phys. Rev. Lett. **51**, 1336 (1983).
[38] M. Möttönen, V. Pietilä, and S. M. M. Virtanen, Phys. Rev. Lett. **99**, 250406 (2007).
[39] A. E. Leanhardt, Ph.D. thesis, MIT (2003).
[40] P. Zhang, H. H. Jen, C. P. Sun, and L. You, Phys. Rev. Lett. **98**, 030403 (2007).
[41] T. L. Ho and V. B. Shenoy, Phys. Rev. Lett. **77**, 2595 (1996).
[42] E. A. Hinds and C. Eberlein, Phys. Rev. A **61**, 033614 (2000).
[43] R. M. Potvliege and V. Zehnlé, Phys. Rev. A **63**, 025601 (2001).
[44] J. Fortágh and C. Zimmermann, Rev. Mod. Phys. **79**, 235 (2007).
[45] I. Lesanovsky, T. Schumm, S. Hofferberth, L. M. Andersson, P. Kruger, and J. Schmiedmayer, Phys. Rev. A **73**, 033619 (2006).
[46] J. Estève *et al.*, Eur. Phys. J. D **35**, 141 (2005).
[47] Y. Kato *et al.*, Science **306**, 1910 (2004).
[48] Y. Kawaguchi, H. Saito, and M. Ueda, Phys. Rev. Lett. **96**, 080405 (2006).
[49] K. Gawryluk, M. Brewczyk, K. Bongs, and M. Gajda, Phys. Rev. Lett. **99**, 130401 (2007).
[50] M. Möttönen, T. Mizushima, T. Isoshima, M. M. Salomaa, and K. Machida, Phys. Rev. A **68**, 023611 (2003).
[51] Y. Shin, M. Saba, M. Vengalattore, T. A. Pasquini, C. Sanner, A. E. Leanhardt, M. Prentiss, D. E. Pritchard, and W. Ketterle, Phys. Rev. Lett. **93**, 160406 (2004).
[52] J. A. M. Huhtamäki, M. Möttönen, T. Isoshima, V. Pietilä, and S. M. M. Virtanen, Phys. Rev. Lett. **97**, 110406 (2006).